Published in final edited form as:

J Neurochem. 2017 December ; 143(6): 736–749. doi:10.1111/jnc.14211.

The conformational epitope for a new Aβ42 protofibril-selective antibody partially overlaps with the peptide N-terminal region

Benjamin A. Colvin[1,‡], **Victoria A. Rogers**[1,‡], **Joshua A. Kulas**[2], **Elizabeth A. Ridgway**[1], **Fatima S. Amtashar**[1], **Colin K. Combs**[2], and **Michael R. Nichols**[*,1]

[1]Department of Chemistry and Biochemistry, University of Missouri-St. Louis

[2]Department of Biomedical Sciences, University of North Dakota, School of Medicine and Health Sciences

Abstract

Aggregation and accumulation of amyloid-β peptide (Aβ) is a key component of Alzheimer's disease (AD). While monomeric Aβ appears to be benign, oligomers adopt a biologically detrimental structure. These soluble structures can be detected in AD brain tissue by antibodies that demonstrate selectivity for aggregated Aβ. Protofibrils are a subset of soluble oligomeric Aβ species and are described as small (<100 nm) curvilinear assemblies enriched in β-sheet structure. Our own in vitro studies demonstrate that microglial cells are much more sensitive to soluble Aβ42 protofibrils compared to Aβ42 monomer or insoluble Aβ42 fibrils. Protofibrils interact with microglia, trigger Toll-like receptor signaling, elicit cytokine transcription and expression, and are rapidly taken up by the cells. Due to the importance of this Aβ species, we sought to develop an antibody that selectively recognizes protofibrils over other Aβ species. Immunization of rabbits with isolated Aβ42 protofibrils generated a high-titer serum with a strong affinity for Aβ42 protofibrils. The anti-serum, termed AbSL, was selective for Aβ42 protofibrils over Aβ42 monomers and Aβ42 fibrils. AbSL did not react with amyloid precursor protein and recognized distinct pathological features in AD transgenic mouse brain slices. Competition studies with an Aβ antibody that targets residues 1-16 indicated that the conformational epitope for AbSL involved the N-terminal region of protofibrils in some manner. The newly-developed antibody may have potential diagnostic and therapeutic uses in AD tissue and patients, and targeting of protofibrils in AD may have beneficial effects.

[*]To whom correspondence should be addressed: Dr. Michael R. Nichols, Department of Chemistry and Biochemistry, University of Missouri-St. Louis, One University Boulevard, St. Louis, Missouri 63121. Telephone: (314) 516-7345. Fax: (314) 516-5342. nicholsmic@umsl.edu.

[‡]denotes an equal contribution by the first two authors

[1]Abbreviations used: AbSL, antibody St. Louis, AD, Alzheimer's disease, Aβ, amyloid-β protein, APP, amyloid precursor protein, aCSF, artificial cerebrospinal fluid, BCA, bicinchoninic acid, BSA, bovine serum albumin, DLS, dynamic light scattering, ELISA, enzyme-linked immunosorbent assay, GuHCl, guanidine hydrochloride, HFIP, hexafluoroisopropanol, HRP, horseradish peroxidase, R_H, hydrodynamic radius, SEC, size exclusion chromatography, TEM, transmission electron microscopy, ThT, thioflavin T.

Involves human subjects: Informed consent & ethics approval achieved: Informed consent was achieved for all subjects, and the experiments were approved by the local ethics committee.

ARRIVE guidelines have been followed: All experiments were conducted in compliance with the ARRIVE guidelines.

Conflicts of interest: The authors have no conflict of interest to declare.

Conflict of interest disclosure: The authors declare that they have no conflict of interests.

Graphical abstract

Protofibrils are a subset of soluble oligomeric amyloid-β (Aβ) species, which interact with microglia, trigger Toll-like receptor signaling, elicit cytokine transcription and expression, and are rapidly taken up by the cells. Due to the importance of this Aβ species, we sought to develop an antibody that selectively recognizes protofibrils over other Aβ species. Immunization of rabbits with isolated Aβ42 protofibrils generated a high-titer serum with a strong affinity for Aβ42 protofibrils. The image shows an area of Aβ accumulation in a brain slice from a 15 month old APP/PS1 mouse. The brain tissue sample was immunostained with Aβ42 protofibril-selective AbSL antiserum (green) and 4G8 monoclonal antibody (red), which is reactive to residues 17-24 of aggregated and unaggregated Aβ. Very little colocalization (yellow) can be seen in this merged image. Notable differences were observed in the response and localization of each antibody indicating areas of Aβ pathology that are uniquely accessible by AbSL. It is hoped that development of conformationally-selective Aβ antibodies will aid in Alzheimer's disease research, diagnostics, and potentially therapeutics.

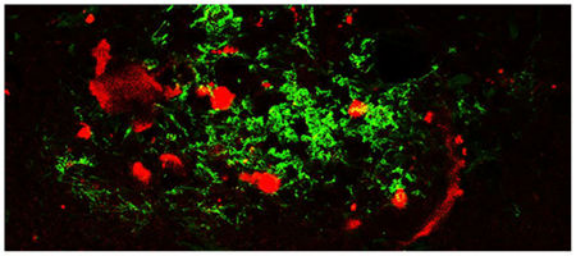

Graphical abstract

Aggregation and accumulation of amyloid-β peptide (Aβ) is a key component of Alzheimer's disease (AD). The aggregation process yields a variety of soluble (protofibrils) and insoluble (fibrils) species. Due to the importance of protofibrils, an anti-serum, termed AbSL, was developed and found to be selective for Aβ protofibrils over monomers and fibrils. The newly-developed antibody may have potential diagnostic and therapeutic uses.

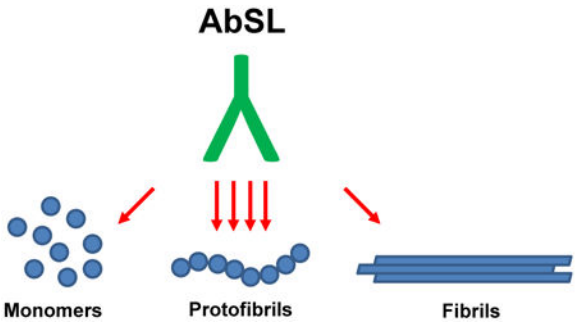

Keywords

Amyloid-beta; conformation-selective antibody; protofibrils

Introduction

Amyloid-β peptide (Aβ) antibodies have been an important tool in Alzheimer's disease research (Masters *et al.* 2016). Many of the first-line antibodies were instrumental in the detection of pathological Aβ hallmarks of the AD brain including neuritic plaques and cerebral deposits (Wong *et al.* 1985). Furthermore, antibodies have allowed quantitative measurement of Aβ levels in human fluids (Seubert *et al.* 1992). Generation of C-terminal-selective Aβ antibodies that distinguish between Aβ40 and Aβ42 helped resolve the composition of Aβ in plaques (Gravina *et al.* 1995). More recently, the advent of conformation-selective antibodies has allowed probing of oligomeric and fibrillar structures *in vitro*, in mouse models, and in human tissues and fluids (Georganopoulou *et al.* 2005; Kayed *et al.* 2007; Deshpande *et al.* 2009; Koffie *et al.* 2009). Increasingly, Aβ antibodies are the primary determinant of structural identification for aggregated species found *in vivo*.

Much of the recent emphasis on soluble Aβ aggregates has been on oligomers, yet much more structural information is known about protofibrils. The first observation and characterization of protofibrils 20 years ago described these small soluble species as enriched in β-sheet structure (Walsh *et al.* 1999) and as precursors to fibrils (Harper *et al.* 1997; Walsh *et al.* 1997). Centrifugation of Aβ solutions followed by size exclusion chromatography of the supernatant has been instrumental in isolating protofibrils for further characterization (Walsh *et al.* 1997; Jan *et al.* 2010). Previous size analyses of protofibrils yielded lengths of typically <200 nm (Harper *et al.* 1997; Walsh *et al.* 1997) and a range of hydrodynamic radii (R_H) values from 10-50 nm (Walsh *et al.* 1997; Paranjape *et al.* 2012; Nichols *et al.* 2015). Structurally, protofibrils have some macroscopic similarities to fibrils based on thioflavin T binding, circular dichroism (Walsh *et al.* 1999) and hydrogen exchange (Kheterpal *et al.* 2003), but have not yet developed the full stability of fibrillar Aβ (Walsh *et al.* 1999; Kheterpal *et al.* 2003). Protofibril diameters are typically smaller than fibrils and range from 4-6 nm although the protofibril to fibril transition can occur without a change in diameter via monomer deposition on protofibril ends or end-to-end annealing of protofibrils (Harper *et al.* 1997; Harper *et al.* 1999). Protofibril conversion to fibrils can also occur by lateral association of protofibrils (Nichols *et al.* 2002). Protofibrils display toxicity to neurons (Walsh *et al.* 1999), disrupt ion channels (Ye *et al.* 2003), inhibit hippocampal long-term potentiation (O'Nuallain *et al.* 2010) and are likely to possess other detrimental biological activities. Protofibrils induce a robust inflammatory response (Paranjape *et al.* 2012; Paranjape *et al.* 2013), initiate Toll-like receptor signaling (Terrill-Usery *et al.* 2014), and are preferentially internalized by microglia (Gouwens *et al.* 2016). Their solubility and diffusible nature quite possibly render them more effective in cellular interactions and engaging microglial receptors compared to mature insoluble fibrils.

Due to the potential role of Aβ42 protofibrils in AD and the ability of these soluble and diffusible protein aggregates to directly impact neuronal viability and stimulate microglial activation, we sought to develop an antibody that selectively recognizes protofibrils. The current report details the generation and characterization of an anti-protofibril serum antibody termed AbSL.

Materials

Resource identifiers

Wild-type (WT) C57BL/6J mice (RRID 000664), APP$^{-/-}$ B6.129S7-App^{tm1Dbo}/J (RRID 004133), and APP/PS1 B6C3-Tg(APPswe, PSEN1dE9)85Dbo/Mmjax (RRID MMRRC_034829-JAX) were obtained from The Jackson Laboratory. Antibodies Y188 (RRID AB_2289606) from Abcam, 22C11 (RRID AB_827115) from Millipore, 4G8 (RRID AB_662812) and 6E10 (RRID AB_1977025) from Biolegend, 6C5 (RRID AB_627679) from Santa Cruz Biotechnology, and Ab9/Ab5 from Mayo Clinic College of Medicine. Mouse IgG2a isotype control (RRID AB_470164) from eBioscience.

Methods

Preparation of Aβ peptides

Aβ42 and Aβ40 peptides were obtained from The ERI Amyloid Laboratory, LLC (Oxford, CT) in lyophilized form and stored at −20 °C. Aβ peptide was dissolved in 100% hexafluoroisopropanol (HFIP) (Sigma-Aldrich, St. Louis) to yield a 1 mmol/L Aβ solution, separated into aliquots in sterile microcentrifuge tubes, and evaporated uncovered at room temperature overnight in a fume hood. The following day the aliquots were vacuum-centrifuged to remove any residual HFIP and stored in desiccant at −20° C. Aβ42 protofibrils were prepared as previously described (Paranjape *et al.* 2012) by dissolving lyophilized Aβ (2 mg) in 50 mmol/L NaOH to yield a 2.5 mmol/L Aβ solution. The solution was then diluted to 250 μmol/L Aβ in prefiltered (0.22 μmol/L) artificial cerebrospinal fluid (aCSF, 15 mmol/L $NaHCO_3$, 1 mmol/L Na_2HPO_4, 130 mmol/L NaCl, 3 mmol/L KCl, pH 7.8), incubated for 15-30 min at room temperature, and centrifuged at 18,000*g* for 10 min with a Beckman-Coulter Microfuge 18 prior to chromatographic analysis of the supernatant. Aβ40 protofibrils were prepared in a similar manner although the Aβ40 solution concentration was 500 μmol/L and the solution was incubated for 72 h at 37 °C. Protofibril preparations also yielded almost 50% Aβ42 monomers for further use. Alternatively, aliquots of Aβ42 were reconstituted in 6 mol/L guanidine hydrochloride (GuHCl) / 10 mmol/L NH_4OH to discourage protofibril formation and increase the yield of monomers for subsequent size exclusion chromatographic purification. Aβ25-35 (0.5 mg) was reconstituted using the GuHCl method and Aβ25-35 monomers were isolated in aCSF. Aβ42 fibrils were prepared from purified Aβ42 monomers by incubation in low retention (siliconized) tubes for 360 h at 4 °C. Fibril formation was confirmed with thioflavin T fluorescence and sedimentation by centrifugation at 18,000*g*. Aggregation of Aβ25-35 (130 μmol/L) was accomplished by shaking a solution of purified Aβ25-35 monomers in a low retention tube on an IKA shaker at 750 rpm for 6 days at 25 °C.

Size exclusion chromatography

Supernatants of Aβ preparations (protofibrillar or monomer) were fractionated on a Superdex 75 HR 10/30 column (GE Healthcare) with a fractionation range of 3-70 kD using an AKTA FPLC system (GE Healthcare). Prior to chromatographic isolation of Aβ, bovine serum albumin (BSA, 5 mg) taken from a sterile 75 g/L fraction V solution (Sigma) was passed over the column to limit non-specific binding of Aβ to the column matrix. Following

sample loading, Aβ was eluted at 0.5 mL min^{-1} in aCSF and 0.5 mL fractions were collected and immediately placed on ice. Aβ42 and Aβ40 concentrations were determined by in-line UV absorbance using an extinction coefficient of 1450 cm^{-1} M^{-1} at 280 nm. Aβ25-35 concentration was determined by bicinchoninic acid (BCA) assay using BSA to construct a standard curve.

Dynamic light scattering

Hydrodynamic radius (R_H) measurements were made at room temperature with a DynaPro Titan instrument (Wyatt Technology, Santa Barbara, CA). Samples (35 μl) were placed directly into a quartz cuvette and light scattering intensity was collected at a 90° angle using a 5-second acquisition time. Particle diffusion coefficients were calculated from auto-correlated light intensity data and converted to R_H with the Stokes-Einstein equation. Mean R_H values were obtained with Dynamics software (version 6.12.03).

Thioflavin T fluorescence

Aβ solutions were assessed by ThT fluorescence as described previously (Nichols *et al.* 2002). SEC Aβ fractions were diluted in aCSF pH 7.8 containing 10 μmol/L ThT. Fluorescence emission scans (460-520 nm) were acquired on a Cary Eclipse fluorescence spectrophotometer using an excitation wavelength of 450 nm. Emission scans were integrated from 470-500 nm to provide a numerical value of ThT relative fluorescence values (RFU).

Electron microscopy

SEC-purified Aβ42 protofibrils and Aβ25-35 aggregates (10 μl) were applied to a 200-mesh formvar-coated copper grid (Ted Pella, Inc.). Samples were allowed to adsorb for 10 min at 25°C, followed by removal of excess sample solution. Grids were washed three times by placing sample side down on a droplet of water. Heavy metal staining was done by incubation of the grid on a droplet of 2% uranyl acetate (Electron Microscopy Sciences, Hatfield, PA) for 5 min, removal of excess solution, and air drying. Affixed samples were visualized with a JEOL JEM-2000 FX transmission electron microscope operated at 200k eV.

Generation of rabbit anti-serum

SEC-purified Aβ42 protofibrils were shipped overnight on ice to Pacific Immunology (Ramona, CA). Pre-immune serum from two New Zealand White rabbits (PAC-10079 and PAC-10080) was obtained prior to their immunization with 0.1 mg Aβ42 protofibrils in Complete Freund's Adjuvant. Three additional immunizations were administered with 0.1 mg Aβ42 protofibrils in Incomplete Freund's Adjuvant. Five separate bleeds and an exsanguination were obtained from each rabbit and shipped to University of Missouri-St. Louis.

Indirect ELISA

Monomeric, protofibrillar, and fibrillar Aβ (0.05 mL/well), prepared at various concentrations, was adsorbed overnight at 4 °C in 0.05 mol/L bicarbonate buffer pH 9.6 on a

Nunc 96-well MaxiSorp flat-bottom immunoplate. The wells were washed with phosphate buffered saline containing 0.05 mL/L Tween 20 (PBST) and then blocked with 150 μL PBST containing 0.1 g/mL milk for 1 h. All steps were done at room temperature with one PBST wash between plating and blocking steps, and four PBST washes performed between primary and secondary antibody steps. Primary antibody (AbSL anti-serum or otherwise) diluted into PBST containing 0.05 g/mL milk (0.1 mL) was added to each well for 1 h followed by 0.1 mL of secondary antibody in PBST containing 0.05 g/mL milk for 2 h. Either an affinity-purified goat anti-rabbit (for AbSL, R&D Systems HAF008, polyclonal, <5% cross-reactivity with human IgG, mouse IgG) or goat anti-mouse (for Ab9, R&D Systems HAF007, polyclonal, <2% cross-reactivity with human IgG, rabbit IgG) IgG-horseradish peroxidase (HRP) conjugate was used. A 1:1 mixture (0.1 mL) of HRP substrate (TMB, 3,3′,5,5′-tetramethylbenzidine and hydrogen peroxide) was incubated in the wells for 2-5 min and the reaction stopped with 0.05 mL 1 mol/L sulfuric acid. The optical density of each sample was obtained at 450 nm with a reference reading subtracted at 630 nm using a SpectraMax 340 absorbance plate reader (Molecular Devices). Antibody competition studies using the indirect ELISA method were conducted in a similar manner but with variations in the type and concentration of primary (AbSL, Ab9, Ab5, mouse IgG isotype control) and secondary antibodies (anti-rabbit IgG-HRP or anti-mouse IgG-HRP).

Dot blot

Dilutions of Aβ42 protofibrils, fibrils, and monomers (2 μL) were applied to a pre-wetted and dried nitrocellulose membrane and allowed to dry for 20 min. The membrane was incubated in blocking buffer (PBST containing 0.1 g/mL milk) on a rotary shaker for 1 h. After washing the membrane for 5 min 3× with PBST, the membrane was incubated with AbSL (1:1000 dilution) under gentle rotation (70 rpm) for 1 h. A second wash step was followed by a 1:1000 dilution of anti-rabbit IgG-HRP antibody for 1 h and a third wash step. The membrane was then treated with Pierce ECL western blotting substrate for 1 min under vigorous rotation (120 rpm). Biomax XAR film was exposed to the membrane and developed.

Western Blot

All animal use was approved by the University of North Dakota Institutional Animal Care and Use Committee (1505-3). Temporal cortex from C57BL/6 (WT), $APP^{-/-}$, and APP/PS1 ((APPswe, PSEN1dE9)85Dbo/ Mjax) mice (Jackson Laboratory) was homogenized in radioimmunoprecipitation assay (RIPA) buffer containing protease inhibitor (Sigma Aldrich P8340) and sodium orthovanadate as a phosphatase inhibitor. The concentration of each protein homogenate was determined using the Bradford method (Bradford 1976). 10 micrograms of each protein sample was then resolved by 0.1 g/mL SDS-PAGE. Proteins were then transferred to PVDF membrane and blocked using a 0.05 g/mL BSA solution for 1 hour before application of primary antibody diluted in 0.05 g/mL BSA. Antibodies against full length c-terminal APP (Y188, Abcam) (22C11, Millipore), Aβ (4G8, Biolegend), human APP/Aβ (6E10, Biolegend), and GAPDH (6C5, Santa Cruz Biotechnology) as a loading control were applied at a 1:1000 dilution overnight at 4° C. AbSL anti-serum was utilized at a 1:5000 dilution in a 0.05 g/mL milk solution overnight at 4 °C. Species-specific HRP-conjugated secondary antibodies were applied to blots for two hours, then blots were

washed with Tris-buffered saline containing 1 mL/L Tween 20 (TBS-T). Blots were visualized using chemiluminescence and images were acquired using an Omega™ Lum G imaging system.

Brain Immunofluorescence

15 month old WT (C57BL/6) or APP/PS1 female animals were euthanized and perfused using sterile Ca^{2+}/PBS solution. Brain hemispheres were collected and chemically crosslinked (fixed) for 24 hr in 4% paraformaldehyde/PBS solution. After 24 hours of fixation, brain hemispheres were then equilibrated 3 times over 3 days in 0.15 g/mL (15%), 0.3 g/mL (30%) and 0.3 g/mL (30%) sucrose-PBS solutions until flotation ceased. Brain hemispheres were then embedded in 0.15 g/mL gelatin and sliced to a thickness of 40 microns using a sliding microtome (Leica). Antigen retrieval was performed on brain sections prior to immunostaining by applying 0.25 g/mL formic acid solution to brain sections for 25 min at room temperature. Immunoflourescent labeling of free-floating brain sections was performed using the 4G8 antibody and AbSL antiserum at a 1:500 dilution in immunostain solution (PBS containing 0.005 g/mL BSA, 1 mL/L Triton X-100, 50 mL/L horse serum and 0.2 g/L sodium azide). Tissue sections were treated with antibodies in solution for 48 hr with gentle mechanical agitation. Sections were then washed with immunostain solution and incubated with AlexaFluor 488-anti-rabbit or AlexaFluor 594-anti-mouse secondary antibodies (ThermoFisher Scientific) for 4 hr at a 1:2000 dilution. Nonspecific secondary antibody staining was determined using secondary antibodies alone without primary antibodies. Following secondary antibody application, tissue was washed two times with immunostain solution and then two times in PBS alone before mounting on glass slides. Tissue was allowed to briefly dry and adhere to slides for 30 min with continuous air flow before application of ProLong Diamond antifade mounting media with DAPI (ThermoFisher Scientific) and coverslips. Sections were visualized using a Leica DMI600B epiflourescent microscope or a Zeiss LSM 510 meta confocal microscope using a 488 nm or 543 nm laser to excite flourophores. Epiflourescent images were compiled as TIFFs for production of figures, while confocal. lsm files were converted to TIFF files using ImageJ software with final figures produced using Photoshop software.

Sandwich ELISA

0.1 ml capture antibodies in PBS (Ab9, 1 μg/ml; Ab2.1.3, 5 μg/ml) were added to wells of a 96-well immunoplate, incubated overnight, washed with PBST, and blocked the next day with 0.3 mL PBST containing 0.1 g/mL milk for 1 h. PBST washes (×3) were done in between each of the following steps. 50 μL Aβ42 protofibrils in aCSF were incubated on the capture antibodies for 2 h, the plate was washed, followed by addition of 0.1 mL of HRP-conjugated or unlabeled detection antibody diluted in PBST containing 0.05 g/mL milk for 2 h. When unlabeled AbSL was used as the primary detection antibody, a secondary HRP-labeled anti-rabbit IgG detection antibody (0.1 mL) was added for an additional 2 h. After a final wash step, 0.1 mL of TMB substrate was added for 2-5 min prior to stopping the reaction with 0.05 mL 1 mol/L sulfuric acid. Absorbance was obtained as described for the indirect ELISA.

Statistical analysis

Data points are presented as mean ± standard error measurement (SEM). Values statistically different from controls were determined using one-way ANOVA when applicable.

Results

Characterization of Aβ42 protofibrils and immunization

Aβ42 protofibrils were prepared and isolated by SEC (Figure 1A) in a modified artificial cerebrospinal fluid buffering system (aCSF) as previously detailed (Paranjape *et al.* 2013). Sufficient amounts (2 mL, 0.2 mg/mL) of protofibrils were obtained and characterized prior to rabbit immunization. Aβ42 protofibrils, which we have previously determined to range in molecular weight from 200-2600 kD (Nichols *et al.* 2015), eluted in the void volume of a Superdex 75 column. These fractions bound thioflavin T (ThT), resulting in a marked increase in 480 nm fluorescence emission (Figure 1B). Protofibrils from the peak SEC fractions were pooled and analyzed by transmission electron microscopy (TEM). Short (<100 nm), curvilinear structures were observed. The size of the protofibrillar species was consistent with earlier dynamic light scattering (DLS) examinations with a mean hydrodynamic radius (R_H) of 18.0 ± 2.5 nm (standard deviation) (Figure 1D). Pre-immune serum was obtained from two rabbits that were subsequently immunized (Pacific Immunology, CA) with Aβ42 protofibrils once in Complete (CFA) and twice in Incomplete Freund's Adjuvant (IFA) over a six week period. Two bleeds were obtained over three weeks followed by a third immunization in IFA and two additional bleeds.

Titer determination of anti-serum and selectivity for Aβ species

The pre-immune serum (PB) and all four bleeds (B1-4) from both rabbits were evaluated for Aβ recognition using an indirect ELISA assay as outlined and depicted in Figure 8A. Aβ42 protofibrils were adsorbed to the wells of a 96-well immunoplate overnight and exposed to increasing dilutions of the rabbit serum. Rabbit #1 (PAC79) displayed high titers for protofibrils within the first bleed and the antibody titer level remained consistent throughout the bleed protocol (Figure 2A). Rabbit #2 (PAC80) was slower to generate antibodies but eventually displayed antibody titers that matched and exceeded those of Rabbit #1 (Figure 2B). Antibody titers were determined to range from 25,000 to >50,000 in the newly characterized antiserum, denoted AbSL antiserum. Serum AbSL titers were also tested against different forms of Aβ42, including protofibrils, monomers, and fibrils (Figure 2C). Curve fitting with a 3-parameter hyperbolic decay produced EC_{50} serum dilution values of 1:542, 1:14, and 1:84 for protofibrils, monomers, and fibrils respectively.

The selectivity for Aβ42 protofibrils by AbSL antiserum was further tested by adsorbing isolated Aβ42 protofibrils, monomers, and fibrils at similar concentration ranges to immunoplates and carrying out an indirect ELISA. Significant selectivity was observed by AbSL antiserum for protofibrils compared to monomers and fibrils at lower mass amounts of Aβ42 (Figure 3A). Extended concentration ranges of the three Aβ42 species (Figure 3B) highlighted the selectivity both in the magnitude and EC_{50} of the response (protofibrils, 59 ng; monomers, 124 ng; fibrils, 2845 ng). A semi-log plot of the extended Aβ concentration data in Figure 3B was used to better emphasize the selectivity differences of AbSL for

distinct Aβ42 species (Figure 3C). Under the same conditions, Ab9, a monoclonal Aβ antibody (IgG2a isotype) of mouse origin that recognizes the peptide N-terminal domain (residues 1-16) and is not conformation-selective (Kukar *et al.* 2005; Levites *et al.* 2006), did not display any selectivity between protofibrils and monomers (Figure 3D). Reactivity to fibrils by Ab9 was decreased somewhat, although not nearly to the same extent as AbSL antiserum. The lower reactivity to fibrils by Ab9 may reflect coverage of some epitopes by the fibril macrostructure (i.e. lateral association of filaments) and is likely not representative of conformational selectivity.

We have previously shown that Aβ40 protofibrils take longer to form, are less stable, and exhibit a reduced ability to induce TNFα secretion in microglia than Aβ42 protofibrils (Paranjape *et al.* 2012). Indirect ELISA analysis of AbSL antiserum reactivity to immunoplate-adsorbed Aβ42 or Aβ40 protofibrils suggested a higher affinity for Aβ42 protofibrils (Figure 3E). Curve fitting with a single rectangular hyperbola equation yielded a value for the amount of Aβ adsorbed at half-maximal binding of 4 ng for Aβ42 protofibrils and 16 ng for Aβ40 protofibrils. Dot blot analysis also demonstrated the selective affinity of AbSL for Aβ42 protofibrils over Aβ42 monomers (Figure 4A) and fibrils (Figure 4B). Ab9 was again used as a positive control in Figure 4A to confirm the presence of Aβ42 monomers on the nitrocellulose membrane.

AbSL does not recognize amyloid precursor protein (APP)

An important criterion for antibodies that are designed to be specific for Aβ is that they don't bind the amyloid precursor protein (APP). APP is an integral membrane protein that yields Aβ after proteolytic cleavage by β and γ secretases (Hardy and Selkoe 2002). Since the Aβ sequence is within APP, there can sometimes be cross-reactivity by antibodies for Aβ and APP. A major band for APP is typically observed around 100 to 130 kilodaltons (Selkoe *et al.* 1988). The temporal cortices of C57BL/6 wild-type (WT), APP knockout ($APP^{-/-}$), and mutant APP/presenilin (APP/PS1) mice were collected and homogenized to yield protein extracts (Zheng *et al.* 1995; Jankowsky *et al.* 2004). Protein homogenates were analyzed by SDS-PAGE/immunoblot to determine reactivity to APP (~110 kD). Membranes were probed with AbSL, anti-APP (C2211 and Y188), anti-Aβ (4G8 and 6E10), and anti-GAPDH antibodies. Robust antibody binding around 110 kD was detected on membranes probed with the 22C11 and Y188 antibodies in WT and APP/PS1 temporal cortex samples, and was absent in $APP^{-/-}$ samples (Figure 5A) supporting their selectivity for APP. The 6E10 monoclonal antibody, which is known to be preferentially selective for human APP, reacted with the human transgenic APP in the APP/PS1 cortex lysate and did not detect mouse APP in WT samples or show binding in APP-/- samples. Full length APP in WT and APP/PS1 cortex homogenates was not detected by the 4G8 antibody. AbSL did not react with the 110 kD band over background (Figure 5A). Similar results were obtained in an additional gel and immunoblotting experiment that also contained an *in vitro*-prepared soluble oligomeric/protofibrillar Aβ42. 22C11 recognized full length APP, but not the Aβ42 species (Figure 5B) as predicted based upon its N-terminal APP epitope. AbSL recognized the Aβ42 species, but not APP. Taken together, these findings indicate that AbSL antiserum is Aβ conformation-selective with little to no APP cross-reactivity.

AbSL recognizes distinct pathological features in APP/PS1 brain tissue

Brain slices from 15 month old APP/PS1 mice were stained with AbSL antiserum and 4G8 monoclonal antibody. 4G8 is reactive to residues 17-24 of aggregated and unaggregated Aβ (Kim *et al.* 1988). Confocal imaging of the brain tissue showed classical plaque-like features that were recognized by both AbSL and 4G8 (Figure 6A). However, significant differences were observed in the response and localization of each antibody. Notably distinct areas were stained by one antibody or the other without colocalization. In many cases AbSL stained fringe areas of the amyloid plaque and had a strong reactivity overall. There were a number of areas that did indicate colocalization by AbSL and 4G8. The confocal microscopy findings in Figure 6A suggested that there were areas of Aβ structure in the pathology that were uniquely accessible by AbSL. Epifluorescence imaging of hippocampal slices obtained from 15 mo APP/PS1 mice (Figure 6B) revealed numerous accumulations that were detected by AbSL but not 4G8. The number and intensity of the accumulations was substantial. The pathology was not observed in 15 mo WT mice (Figure 6C). Both types of fluorescence imaging highlighted the robust staining capability of AbSL.

Epitope competition between AbSL and other Aβ antibodies

The analysis provided strong evidence for AbSL recognition of a conformational epitope present on Aβ42 protofibrils. In order to gain further information on the AbSL epitope on protofibrils, AbSL binding was assessed by indirect ELISA competition studies with Ab9 (anti-$Aβ_{1-16}$ mAb of IgG2a isotype) or Ab5 (anti-$Aβ_{1-16}$ mAb of IgG2b isotype). Ab9 and Ab5 are from the same antibody lineage and have the same epitope. Aβ42 protofibrils were coated onto an immunoplate followed by application of antibody mixtures containing AbSL (at a fixed dilution) and Ab9 (increasing concentration). The binding of AbSL was monitored by an anti-rabbit IgG-HRP secondary antibody. The data showed that increasing amounts of Ab9 blocked AbSL binding to protofibrils up to a certain point and then had no additional effect (Figure 7A, circles). Application of Ab9 alone to the protofibrils at the same concentrations served as a control measurement and was detected by an anti-mouse IgG-HRP secondary antibody (Figure 7A, diamonds). Ab9 alone was undetectable by the anti-rabbit IgG-HRP secondary antibody (Figure 7A) demonstrating that the anti-rabbit IgG-HRP secondary antibody only monitored AbSL binding to the protofibrils.

Reverse competition experiments were also conducted in which pre-mixed primary antibody solutions contained varied AbSL dilutions with a fixed Ab5 concentration. Multiple experiments at different fixed Ab5 concentrations indicated that an increase in the Ab5 concentration affected AbSL/Aβ42 protofibril binding (Figure 7B). Curve fitting with a 3-parameter single rectangular hyperbola produced EC_{50} serum dilution values of 1:620 for AbSL alone, 1:534 for AbSL + 1:10,000 Ab5, 1:247 for AbSL + 1:2,000 Ab5, and 1:151 for AbSL + 1:1,000 Ab5 (Figure 7B). Thus, increased Ab5 concentration lowered the response and the affinity of AbSL for Aβ42 protofibrils. However, the effect was finite and leveled out at fixed Ab5 dilutions less than 1:2,000. In a separate experiment, a mouse IgG2a isotype control antibody for Ab5 used at the highest Ab5 concentration (1:1000, 1.4 μg/mL) had no effect on AbSL affinity for Aβ42 protofibrils (data not shown). The competition findings indicated that the AbSL conformational epitope and the Ab9/Ab5 linear sequence epitope were distinct but with some potential regions of overlap.

The possibility that the AbSL conformational epitope on Aβ42 protofibrils may involve the N-terminal region of the peptide was further probed by direct and indirect sandwich ELISA (Figure 8A). Aβ antibodies Ab9 (or Ab5) and Ab2.1.3, a C-terminal Aβ42-selective antibody (Kukar *et al.* 2005), were used as capture antibodies for Aβ42 protofibrils in the sandwich ELISA. The capture antibodies were tested in combination with detection antibody Ab5 conjugated to HRP (Ab5-HRP) in a direct sandwich ELISA or detection antibody AbSL and anti-rabbit IgG-HRP in an indirect sandwich ELISA. The combination of the Aβ42 C-terminal-selective antibody Ab2.1.3 to capture the protofibrils and the N-terminal-selective Ab5-HRP to detect the protofibrils produced a final ELISA absorbance ($OD_{450\ nm}$) well above background (Figure 8B). Capture with Ab2.1.3 and detection with AbSL also yielded a significant $OD_{450\ nm}$ above background levels. This finding suggested that the protofibril epitope for AbSL did not overlap with the C-terminal end of Aβ42. Capture with Ab9 and detection with Ab5-HRP yielded a negligible $OD_{450\ nm}$, consistent with both antibodies recognizing and competing for the same epitope. Capture with Ab9 and detection with AbSL, though, produced a significant $OD_{450\ nm}$ signal relative to background. This result indicated that while indications of overlap were noted, there were distinctions between the two antibody binding sites. The partial overlap between the N-terminal Ab9 epitope and the AbSL conformational protofibril epitope was again observed with the Ab9/AbSL $OD_{450\ nm}$ less than that of Ab2.1.3/AbSL (Figure 8B). However, when varying the AbSL detection antibody dilution after capture of Aβ42 protofibrils by either C-terminal Ab2.1.3 or N-terminal Ab5, the response curves appeared similar (Figure 8C). Curve-fitting indicated the Ab5/AbSL combination to be more sensitive with an EC_{50} at a greater dilution (1:1581) compared to the Ab2.1.3/AbSL combination (1:473). Overall, competition between AbSL and N-terminal antibodies Ab9/Ab5 for Aβ42 protofibrils was less evident in the sandwich ELISA compared to the indirect ELISA.

Aβ42 protofibril standard curves were examined using an indirect sandwich ELISA format to further distinguish the AbSL conformational epitope from the sequence-dependent N-terminal Ab9 epitope. A characteristic binding curve was observed over a concentration range of Aβ42 protofibrils when immunoplates were coated with the Aβ42 C-terminal-selective antibody Ab2.1.3 (capture antibody) followed by AbSL (detection antibody) and anti-rabbit IgG-HRP (Figure 9A). Although the $A_{450\ nm}$ was diminished when Ab9 was used as the capture antibody, the shape and sensitivity of the AbSL binding curve to protofibrils was similar to Ab2.1.3. Curve-fitting confirmed this observation with EC_{50} values of 3.5 ng Aβ and 2.4 ng Aβ for capture antibodies Ab2.1.3 and Ab9 respectively. The findings were indicative of a conformationally distinct site for AbSL that may involve the N-terminal Aβ domain. The sandwich ELISA findings also emphasized the capability of AbSL as a sensitive detection antibody.

Additional analysis utilized an Aβ peptide fragment, Aβ25-35, which contains only the hydrophobic C-terminal region of Aβ. SEC-purified monomers were aggregated under vigorous shaking conditions and displayed ThT fluorescence after 6 days (Figure 10A). The ThT-positive material was sedimented by centrifugation of the solution at 18,000*g*. The Aβ25-35 fibril pellet was isolated and analyzed by TEM (Figure 10B). Thick bundles of relatively short (200-400 nm) rod-like structures were observed. However, neither Aβ25-35 fibrils, nor Aβ25-35 monomers were detected by AbSL anti-serum (Figure 10C). The

Aβ25-35 fibrils and monomers were also not detected by the N-terminal Ab9 antibody (data not shown). These findings demonstrated that ThT binding or fibril formation was not completely sufficient for AbSL recognition and that Aβ protofibrils possess a particular distinct conformation that appears to involve the Aβ N-terminal region in some manner. The absence of N-terminal and C-terminal Aβ segments within Aβ25-35 may also contribute to the lack of recognition by AbSL.

Discussion

This report describes a new serum antibody that is selective for Aβ42 protofibrils and provides further information on the organization of the protofibril epitope. There are numerous antibodies that are reported to be selective for soluble Aβ aggregates. The antibody that is most similar to AbSL is mAb158, a protofibril-specific monoclonal IgG2a antibody generated by immunization of mice with protofibrils prepared from Aβ42 E22G (Arctic mutation) (Englund *et al.* 2007). As with AbSL antiserum, selectivity was observed for mAb158 between protofibrils and monomers. BAN2401 is a humanized IgG1 version of mAb158, has the same binding characteristics as mAb158 (Lannfelt *et al.* 2014), and is currently in clinical trials as a potential AD therapeutic (Logovinsky *et al.* 2016). The Aβ42 Arctic protofibrils in the mAb158 study (Englund *et al.* 2007) appear larger than those prepared from WT Aβ42 both in that report and the protofibrils used here in the current study for AbSL generation (Figure 1). This may explain the observed selectivity by AbSL for protofibrils over fibrils while mAb158 was less able to distinguish between the two Aβ species. Although there is likely to be high structural similarity between protofibrils prepared in different laboratories, there are also possibilities for subtle differences between preparations and somewhat different antibody properties. Therefore, it is expected that there may be differences in affinity and binding sites between similar Aβ conformational-selective antibodies.

A well-recognized conformational-specific antibody that targets oligomers of Aβ and other amyloid proteins is A11 (Kayed *et al.* 2003). A11 displays significant selectivity for oligomers over both monomeric and fibrillar Aβ. However, little structural information is known about oligomers and thus the conformational epitope for A11 has not been fully elucidated. Even to this day, biophysical analyses have yet to completely resolve all the structural similarities and differences between soluble oligomers and protofibrils. A11 has been used to detect oligomers in brain tissue from AD mouse models (Lesne *et al.* 2006; Deshpande *et al.* 2009).

NAB61 is a monoclonal antibody that preferentially recognizes a conformational epitope present in dimeric, small oligomeric, and higher order Aβ structures including plaques in human AD brain tissue (Lee *et al.* 2006). NAB61 was an important component in determining that senile plaques in an AD mouse model were surrounded by a halo of oligomeric Aβ (Koffie *et al.* 2009).

M93 and M94 antibodies were obtained from rabbits immunized with solutions of Aβ-derived diffusible ligands (ADDLs), an oligomeric form of Aβ (Lambert *et al.* 2001). The two polyclonal antibodies were conformational-selective in that they bound Aβ42 ADDLs

with a much higher affinity than Aβ42 monomers. M93 and M94 also bound higher order Aβ species including amyloid fibrils. M93 detected an oligomeric species similar to ADDLs in human AD brain extracts (Lambert *et al.* 2001). Interestingly, solanezumab (m266), another conformation-selective Aβ antibody, binds effectively to oligomeric Aβ and has high affinity for monomeric Aβ, but does not bind fibrils (reviewed in Goure *et al.* 2014).

Several published reports have demonstrated the involvement of the Aβ N-terminal region in the recognition of Aβ by conformational-selective antibodies. Meli et al. generated anti-Aβ recombinant single chain Fv fragment (scFv) antibodies with a high affinity for Aβ oligomers compared to Aβ monomers that also had a preference for the N-terminus or C-terminus (Meli *et al.* 2009). The Aβ epitope for monoclonal antibody PFA1 comprises N-terminal residues 3-6, yet the antibody has a higher affinity for Aβ fibrils and protofibrils than for monomers (Gardberg *et al.* 2007; Gardberg *et al.* 2009). This finding suggested that a combination of conformation and sequence elements involving the Aβ N-terminal region were integral in antibody recognition. A thorough analysis of 23 monoclonal conformationally-selective OC antibodies by Glabe and coworkers found that 17 of the antibodies recognize a linear segment in the Aβ N-terminus (Hatami *et al.* 2014). These studies, and the current work with AbSL, indicate that there may be some sort of structural framework within the N-terminal region, which was previously thought to be conformationally flexible. The findings from this report on AbSL suggest a partial overlap between the Aβ42 protofibril conformational epitope and the Aβ42 N-terminal sequence.

AbSL, an Aβ42 protofibril-selective antiserum, shows promise as a tool for detecting, targeting and regulating Aβ protofibrils. Serum antibodies have limitations, thus affinity purification and monoclonal development of AbSL antibodies may increase effectiveness and selectivity. Conformation-specific antibodies in Alzheimer's disease have research, diagnostic, and therapeutic applicability. They are currently the best option for analyzing human and mouse model samples and, in some cases, may confirm the physiological existence of particular Aβ forms or structures. There are a number of antibody-based immunotherapies targeting Aβ currently in clinical trials (Cummings *et al.* 2016) and this strategy may be improved by antibodies that are selective for a particular Aβ conformation.

Involves human subjects:

If yes: Informed consent & ethics approval achieved:

=> if yes, please ensure that the info “Informed consent was achieved for all subjects, and the experiments were approved by the local ethics committee.” is included in the Methods

.

ARRIVE guidelines have been followed:

Yes

```
=> if No or if it is a Review or Editorial, skip complete sentence => if
Yes, insert “All experiments were conducted in compliance with the ARRIVE
guidelines.” unless it is a Review or Editorial

Conflicts of interest: none

=> if ‘none’, insert “The authors have no conflict of interest to declare.”

=> otherwise insert info unless it is already included
```

Acknowledgments

We would like to thank the Microscopy Image and Spectroscopy Technology Laboratory in the Center for Nanoscience at University of Missouri-St. Louis for TEM imaging. This work was supported by the following awards: University of Missouri-St. Louis (UMSL) College of Arts & Sciences (CAS) Faculty Research Award (MRN); UMSL CAS Undergraduate Research Award (VAR); UMSL Graduate School Dissertation Fellowship (BAC); and National Institutes of Health 5R01AG042819 (CKC). Confocal microscopy of brain sections was performed with the assistance of the University of North Dakota Imaging Core supported by NIH COBRE 5P30GM103329.

References

Bradford MM. A rapid and sensitive method for the quantitation of microgram quantities of protein utilizing the principle of protein-dye binding. Anal Biochem. 1976; 72:248–254. [PubMed: 942051]

Cummings J, Morstorf T, Lee G. Alzheimer's drug-development pipeline: 2016. Alzheimers Dement. 2016; 2:222–232.

Deshpande A, Kawai H, Metherate R, Glabe CG, Busciglio J. A role for synaptic zinc in activity-dependent Aβ oligomer formation and accumulation at excitatory synapses. J Neurosci. 2009; 29:4004–4015. [PubMed: 19339596]

Englund H, Sehlin D, Johansson AS, Nilsson LN, Gellerfors P, Paulie S, Lannfelt L, Pettersson FE. Sensitive ELISA detection of amyloid-beta protofibrils in biological samples. J Neurochem. 2007; 103:334–345. [PubMed: 17623042]

Gardberg A, Dice L, Pridgen K, Ko J, Patterson P, Ou S, Wetzel R, Dealwis C. Structures of Aβ-related peptide-monoclonal antibody complexes. Biochemistry. 2009; 48:5210–5217. [PubMed: 19385664]

Gardberg AS, Dice LT, Ou S, Rich RL, Helmbrecht E, Ko J, Wetzel R, Myszka DG, Patterson PH, Dealwis C. Molecular basis for passive immunotherapy of Alzheimer's disease. Proc Natl Acad Sci USA. 2007; 104:15659–15664. [PubMed: 17895381]

Georganopoulou DG, Chang L, Nam JM, Thaxton CS, Mufson EJ, Klein WL, Mirkin CA. Nanoparticle-based detection in cerebral spinal fluid of a soluble pathogenic biomarker for Alzheimer's disease. Proc Natl Acad Sci USA. 2005; 102:2273–2276. [PubMed: 15695586]

Goure WF, Krafft GA, Jerecic J, Hefti F. Targeting the proper amyloid-beta neuronal toxins: a path forward for Alzheimer's disease immunotherapeutics. Alzheimers Res Ther. 2014; 6:42. [PubMed: 25045405]

Gouwens LK, Makoni NJ, Rogers VA, Nichols MR. Amyloid-β42 protofibrils are internalized by microglia more extensively than monomers. Brain Res. 2016; 1648:485–495. [PubMed: 27531183]

Gravina SA, Ho L, Eckman CB, Long KE, Otvos L Jr, Younkin LH, Suzuki N, Younkin SG. Amyloid β protein (Aβ) in Alzheimer's disease brain. Biochemical and immunocytochemical analysis with antibodies specific for forms ending at Aβ40 or Aβ42(43). J Biol Chem. 1995; 270:7013–7016. [PubMed: 7706234]

Hardy J, Selkoe DJ. The amyloid hypothesis of Alzheimer's disease: progress and problems on the road to therapeutics. Science. 2002; 297:353–356. [PubMed: 12130773]

Harper JD, Wong SS, Lieber CM, Lansbury PT Jr. Observation of metastable Aβ amyloid protofibrils by atomic force microscopy. Chem Biol. 1997; 4:119–125. [PubMed: 9190286]

Harper JD, Wong SS, Lieber CM, Lansbury PT Jr. Assembly of Aβ amyloid peptides: an *in vitro* model for a possible early event in Alzheimer's disease. Biochemistry. 1999; 38:8972–8980. [PubMed: 10413470]

Hatami A, Albay R 3rd, Monjazeb S, Milton S, Glabe C. Monoclonal antibodies against Aβ42 fibrils distinguish multiple aggregation state polymorphisms *in vitro* and in Alzheimer disease brain. J Biol Chem. 2014; 289:32131–32143. [PubMed: 25281743]

Jan A, Hartley DM, Lashuel HA. Preparation and characterization of toxic Aβ aggregates for structural and functional studies in Alzheimer's disease research. Nat Protoc. 2010; 5:1186–1209. [PubMed: 20539293]

Jankowsky JL, Fadale DJ, Anderson J, Xu GM, Gonzales V, Jenkins NA, Copeland NG, Lee MK, Younkin LH, Wagner SL, Younkin SG, Borchelt DR. Mutant presenilins specifically elevate the levels of the 42 residue β-amyloid peptide *in vivo*: evidence for augmentation of a 42-specific γ secretase. Hum Mol Genet. 2004; 13:159–170. [PubMed: 14645205]

Kayed R, Head E, Thompson JL, McIntire TM, Milton SC, Cotman CW, Glabe CG. Common structure of soluble amyloid oligomers implies common mechanism of pathogenesis. Science. 2003; 300:486–489. [PubMed: 12702875]

Kayed R, Head E, Sarsoza F, Saing T, Cotman CW, Necula M, Margol L, Wu J, Breydo L, Thompson JL, Rasool S, Gurlo T, Butler P, Glabe CG. Fibril specific, conformation dependent antibodies recognize a generic epitope common to amyloid fibrils and fibrillar oligomers that is absent in prefibrillar oligomers. Mol Neurodegener. 2007; 2:18. [PubMed: 17897471]

Kheterpal I, Lashuel HA, Hartley DM, Walz T, Lansbury PT Jr, Wetzel R. Aβ protofibrils possess a stable core structure resistant to hydrogen exchange. Biochemistry. 2003; 42:14092–14098. [PubMed: 14640676]

Kim KS, Miller DL, Sapienza VJ, Chen CMJ, Bai C, Grundke-Iqbal I, Currie JR, Wisniewski HM. Production and characterization of monoclonal antibodies reactive to synthetic cerebrovascular amyloid protein. Neurosci Res Commun. 1988; 2:121–130.

Koffie RM, Meyer-Luehmann M, Hashimoto T, Adams KW, Mielke ML, Garcia-Alloza M, Micheva KD, Smith SJ, Kim ML, Lee VM, Hyman BT, Spires-Jones TL. Oligomeric amyloid β associates with postsynaptic densities and correlates with excitatory synapse loss near senile plaques. Proc Natl Acad Sci USA. 2009; 106:4012–4017. [PubMed: 19228947]

Kukar T, Murphy MP, Eriksen JL, Sagi SA, Weggen S, Smith TE, Ladd T, Khan MA, Kache R, Beard J, Dodson M, Merit S, Ozols VV, Anastasiadis PZ, Das P, Fauq A, Koo EH, Golde TE. Diverse compounds mimic Alzheimer disease-causing mutations by augmenting Aβ42 production. Nat Med. 2005; 11:545–550. [PubMed: 15834426]

Lambert MP, Viola KL, Chromy BA, Chang L, Morgan TE, Yu J, Venton DL, Krafft GA, Finch CE, Klein WL. Vaccination with soluble Aβ oligomers generates toxicity-neutralizing antibodies. J Neurochem. 2001; 79:595–605. [PubMed: 11701763]

Lannfelt L, Moller C, Basun H, Osswald G, Sehlin D, Satlin A, Logovinsky V, Gellerfors P. Perspectives on future Alzheimer therapies: Amyloid-β protofibrils - a new target for immunotherapy with BAN2401 in Alzheimer's disease. Alzheimers Res Ther. 2014; 6:16. [PubMed: 25031633]

Lee EB, Leng LZ, Zhang B, Kwong L, Trojanowski JQ, Abel T, Lee VM. Targeting amyloid-β peptide (Aβ) oligomers by passive immunization with a conformation-selective monoclonal antibody improves learning and memory in Aβ precursor protein (APP) transgenic mice. J Biol Chem. 2006; 281:4292–4299. [PubMed: 16361260]

Lesne S, Koh MT, Kotilinek L, Kayed R, Glabe CG, Yang A, Gallagher M, Ashe KH. A specific amyloid-β protein assembly in the brain impairs memory. Nature. 2006; 440:352–357. [PubMed: 16541076]

Levites Y, Das P, Price RW, Rochette MJ, Kostura LA, McGowan EM, Murphy MP, Golde TE. Anti-$A\beta_{42}$- and anti-$A\beta_{40}$-specific mAbs attenuate amyloid deposition in an Alzheimer disease mouse model. J Clin Invest. 2006; 116:193–201. [PubMed: 16341263]

Logovinsky V, Satlin A, Lai R, Swanson C, Kaplow J, Osswald G, Basun H, Lannfelt L. Safety and tolerability of BAN2401 - a clinical study in Alzheimer's disease with a protofibril selective Aβ antibody. Alzheimers Res Ther. 2016; 8:14. [PubMed: 27048170]

Masters CL, Bateman R, Blennow K, Rowe CC, Sperling RA, Cummings JL. Alzheimer's disease. Nat Rev Dis Primers. 2016; 1:15056.

Meli G, Visintin M, Cannistraci I, Cattaneo A. Direct in vivo intracellular selection of conformation-sensitive antibody domains targeting Alzheimer's amyloid-β oligomers. J Mol Biol. 2009; 387:584–606. [PubMed: 19361429]

Nichols MR, Colvin BA, Hood EA, Paranjape GS, Osborn DC, Terrill-Usery SE. Biophysical comparison of soluble amyloid-β(1-42) protofibrils, oligomers, and protofilaments. Biochemistry. 2015; 54:2193–2204. [PubMed: 25756466]

Nichols MR, Moss MA, Reed DK, Lin WL, Mukhopadhyay R, Hoh JH, Rosenberry TL. Growth of β-amyloid(1-40) protofibrils by monomer elongation and lateral association. Characterization of distinct products by light scattering and atomic force microscopy. Biochemistry. 2002; 41:6115–6127. [PubMed: 11994007]

O'Nuallain B, Freir DB, Nicoll AJ, Risse E, Ferguson N, Herron CE, Collinge J, Walsh DM. Amyloid β-protein dimers rapidly form stable synaptotoxic protofibrils. J Neurosci. 2010; 30:14411–14419. [PubMed: 20980598]

Paranjape GS, Gouwens LK, Osborn DC, Nichols MR. Isolated amyloid-β(1-42) protofibrils, but not isolated fibrils, are robust stimulators of microglia. ACS Chem Neurosci. 2012; 3:302–311. [PubMed: 22860196]

Paranjape GS, Terrill SE, Gouwens LK, Ruck BM, Nichols MR. Amyloid-β(1-42) protofibrils formed in modified artificial cerebrospinal fluid bind and activate microglia. J Neuroimmune Pharmacol. 2013; 8:312–322. [PubMed: 23242692]

Selkoe DJ, Podlisny MB, Joachim CL, Vickers EA, Lee G, Fritz LC, Oltersdorf T. β-Amyloid precursor protein of Alzheimer disease occurs as 110- to 135-kilodalton membrane-associated proteins in neural and nonneural tissues. Proc Natl Acad Sci USA. 1988; 85:7341–7345. [PubMed: 3140239]

Seubert P, Vigo-Pelfrey C, Esch F, Lee M, Dovey H, Davis D, Sinha S, Schlossmacher M, Whaley J, Swindlehurst C, McCormack R, Wolfert R, Selkoe DJ, Lieberberg I, Schenk D. Isolation and quantification of soluble Alzheimer's β-peptide from biological fluids. Nature. 1992; 359:325–327. [PubMed: 1406936]

Terrill-Usery SE, Mohan MJ, Nichols MR. Amyloid-β(1-42) protofibrils stimulate a quantum of secreted IL-1β despite significant intracellular IL-1β accumulation in microglia. Biochim Biophys Acta. 2014; 1842:2276–2285. [PubMed: 25125050]

Terrill-Usery SE, Colvin BA, Davenport RE, Nichols MR. Aβ40 has a subtle effect on Aβ42 protofibril formation, but to a lesser degree than Aβ42 concentration, in Aβ42/Aβ40 mixtures. Arch Biochem Biophys. 2016; 597:1–11. [PubMed: 27013205]

Walsh DM, Lomakin A, Benedek GB, Condron MM, Teplow DB. Amyloid β-protein fibrillogenesis: Detection of a protofibrillar intermediate. J Biol Chem. 1997; 272:22364–22372. [PubMed: 9268388]

Walsh DM, Hartley DM, Kusumoto Y, Fezoui Y, Condron MM, Lomakin A, Benedek GB, Selkoe DJ, Teplow DB. Amyloid β-protein fibrillogenesis: Structure and biological activity of protofibrillar intermediates. J Biol Chem. 1999; 274:25945–25952. [PubMed: 10464339]

Wong CW, Quaranta V, Glenner GG. Neuritic plaques and cerebrovascular amyloid in Alzheimer disease are antigenically related. Proc Natl Acad Sci USA. 1985; 82:8729–8732. [PubMed: 2934737]

Ye CP, Selkoe DJ, Hartley DM. Protofibrils of amyloid β-protein inhibit specific K+ currents in neocortical cultures. Neurobiol Dis. 2003; 13:177–190. [PubMed: 12901832]

Zheng H, Jiang M, Trumbauer ME, Sirinathsinghji DJ, Hopkins R, Smith DW, Heavens RP, Dawson GR, Boyce S, Conner MW, Stevens KA, Slunt HH, Sisoda SS, Chen HY, Van der Ploeg LH. β-Amyloid precursor protein-deficient mice show reactive gliosis and decreased locomotor activity. Cell. 1995; 81:525–531. [PubMed: 7758106]

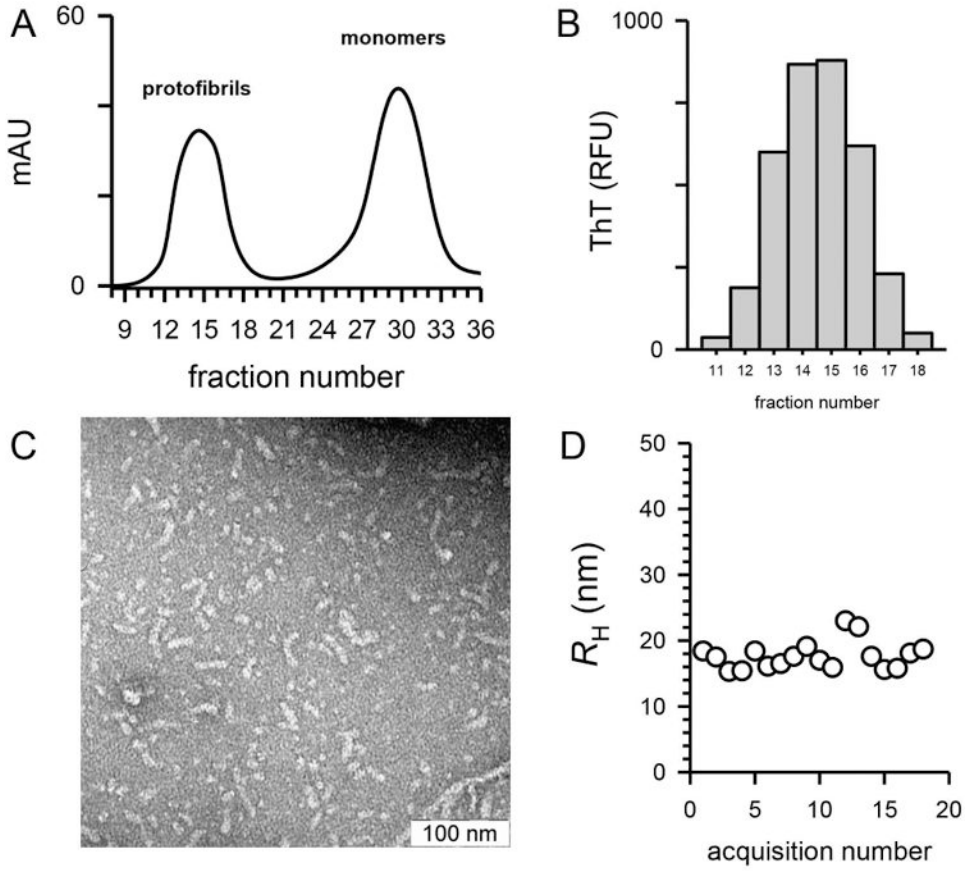

Figure 1.

Characterization of Aβ42 protofibrils used for immunization. Panel A. Aβ42 protofibrils were generated as described in the Methods and isolated on a Superdex 75 SEC column in aCSF. UV absorbance at 280 nm was monitored during the elution (solid line). Panel B. Protofibril SEC fractions (0.5 ml) were diluted by 10 into aCSF containing 5 μmol/L ThT and fluorescence emission was measured as described in the Methods. Panel C. Fractions 13-16 were pooled to yield 2 mL of 42 μmol/L protofibrils. A sample (10 μl) was applied to a copper formvar grid, and imaged by TEM at a magnification of 50,000. The scale bar represents 100 nm. Panel D. Mean R_H was measured by DLS of the Aβ42 protofibril pool and a plot of R_H vs acquisition number is shown.

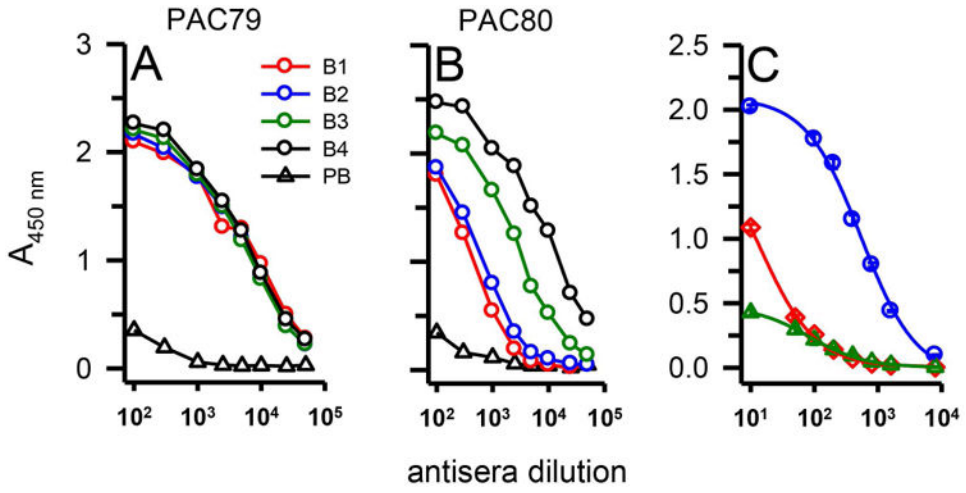

Figure 2.

Serum antibody titer determination for Aβ42 protofibrils. Serum from a pre-bleed (PB) and multiple bleeds (B1-4) of two rabbits (PAC79, Panel A; PAC80, Panel B) immunized with Aβ42 protofibrils was analyzed via indirect ELISA. 96-well ELISA plates were coated with Aβ42 protofibrils (18 ng/well) and treated with increasing dilutions of anti-serum and anti-rabbit IgG-HRP. Each data point represents the average of n=4 trials. Panel C. Varying dilutions of serum antibody were used to detect 18 ng/well of Aβ42 protofibrils (blue circles), Aβ42 monomers (red diamonds), or Aβ42 fibrils (green triangles) by indirect ELISA. Data points (± standard error measurement, SEM) represents the average of n=3 trials and were fit to a 3-parameter hyperbolic decay equation using SigmaPlot software.

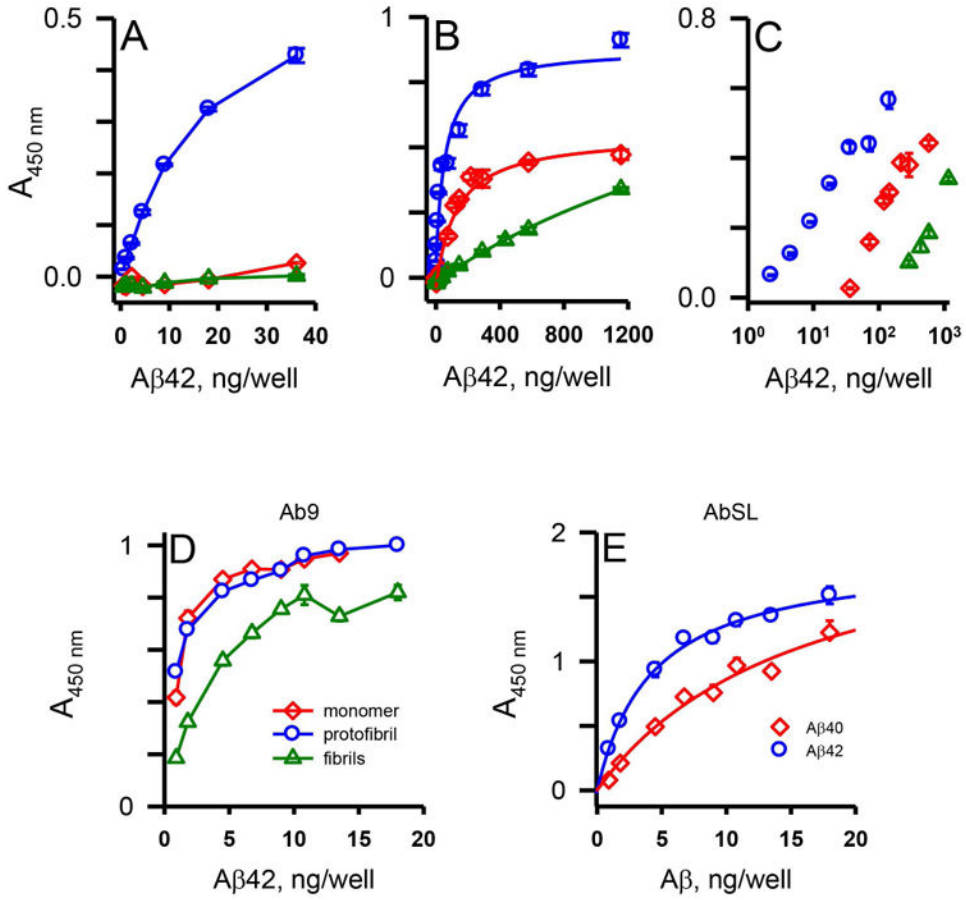

Figure 3.

AbSL antiserum displays selectivity for Aβ42 protofibrils. 96-well ELISA plates were coated with varying amounts of Aβ42 protofibrils, Aβ42 monomers, and Aβ42 fibrils (0.5-1156 ng/well) and analyzed by indirect ELISA with AbSL anti-serum (1:10,000 dilution) and anti-rabbit IgG-HRP (Panels A-C). Panel A depicts the lower Aβ42 concentrations and Panel B shows the extended Aβ42 concentration range. Data in Panel B were fit to a 3-parameter single rectangular hyperbola equation using SigmaPlot software. Data points (± SEM) represent the average of n=3 trials. Panel C is a semi-log re-plot of the central data from Panel B. Panel D. Plates coated with Aβ42 protofibrils, Aβ42 monomers, and Aβ42 fibrils were treated with the N-terminal Aβ antibody Ab9 (1:5,000 dilution) and anti-mouse IgG-HRP. Panel E. Aβ42 protofibrils and Aβ40 protofibrils were prepared separately by different protocols and isolated by SEC. 96-well ELISA plates were coated with a concentration range of protofibrils (0.9-18 ng per well) and analyzed by indirect ELISA. Wells were incubated with AbSL (1:1,000 dilution) followed by anti-rabbit IgG-HRP secondary antibody. Curve-fitting of the data points was performed using SigmaPlot software. Error bars depict SEM for n = 3 wells.

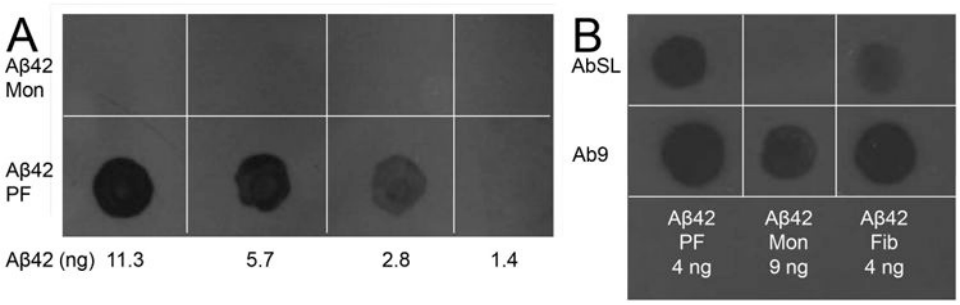

Figure 4.

AbSL antiserum displays selectivity in dot blot assay. Nitrocellulose membranes were spotted with 2 μL Aβ42 monomers, Aβ42 protofibrils, or Aβ42 fibrils (1.4-11 ng) and analyzed by immuno-dot blot. Panel A. Aβ42 monomers and protofibrils were applied at varying concentration to nitrocellulose and treated with AbSL (1:1,000 dilution) and anti-rabbit IgG-HRP secondary antibody as outlined in the Methods. Panel B. Two separate nitrocellulose membranes were spotted with identical samples of Aβ42 monomers, protofibrils, and fibrils. The membranes were incubated with either AbSL (1:1,000 dilution) followed by anti-rabbit IgG-HRP secondary antibody or Ab9 (1:1,000) followed by anti-mouse IgG-HRP secondary antibody.

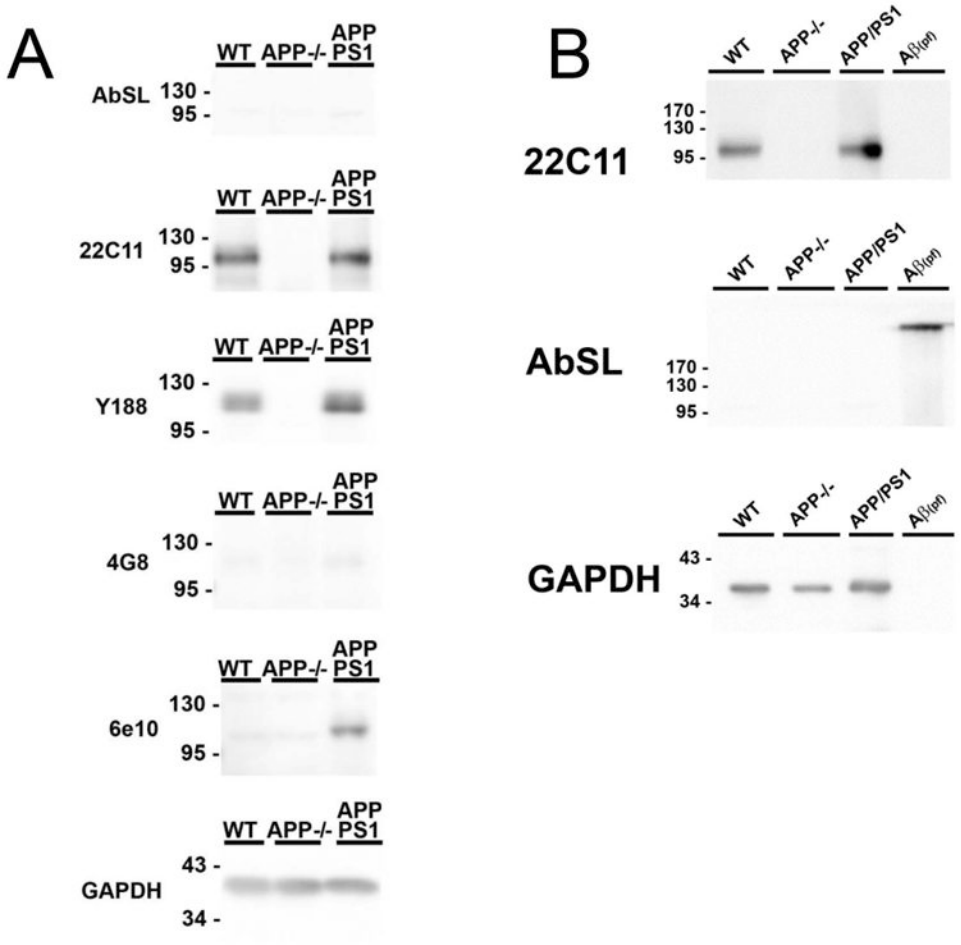

Figure 5.

AbSL antiserum does not recognize APP. Panel A. 10 micrograms of mouse temporal cortex lysate was resolved by SDS-PAGE and transferred to PVDF membranes for western blot. Antibodies against full-length APP (22C11, Y188), Aβ (4G8), human APP/Aβ (6E10) were utilized to detect full length APP and Aβ in samples, while GAPDH was utilized as a loading control. Panel B. Mouse temporal cortex lysate and fibrillized/oligomeric recombinant Aβ peptide were resolved by SDS-PAGE and transferred to PVDF membranes for western blot. Membranes were probed with antibodies against full length APP (22C11) or AbSL.

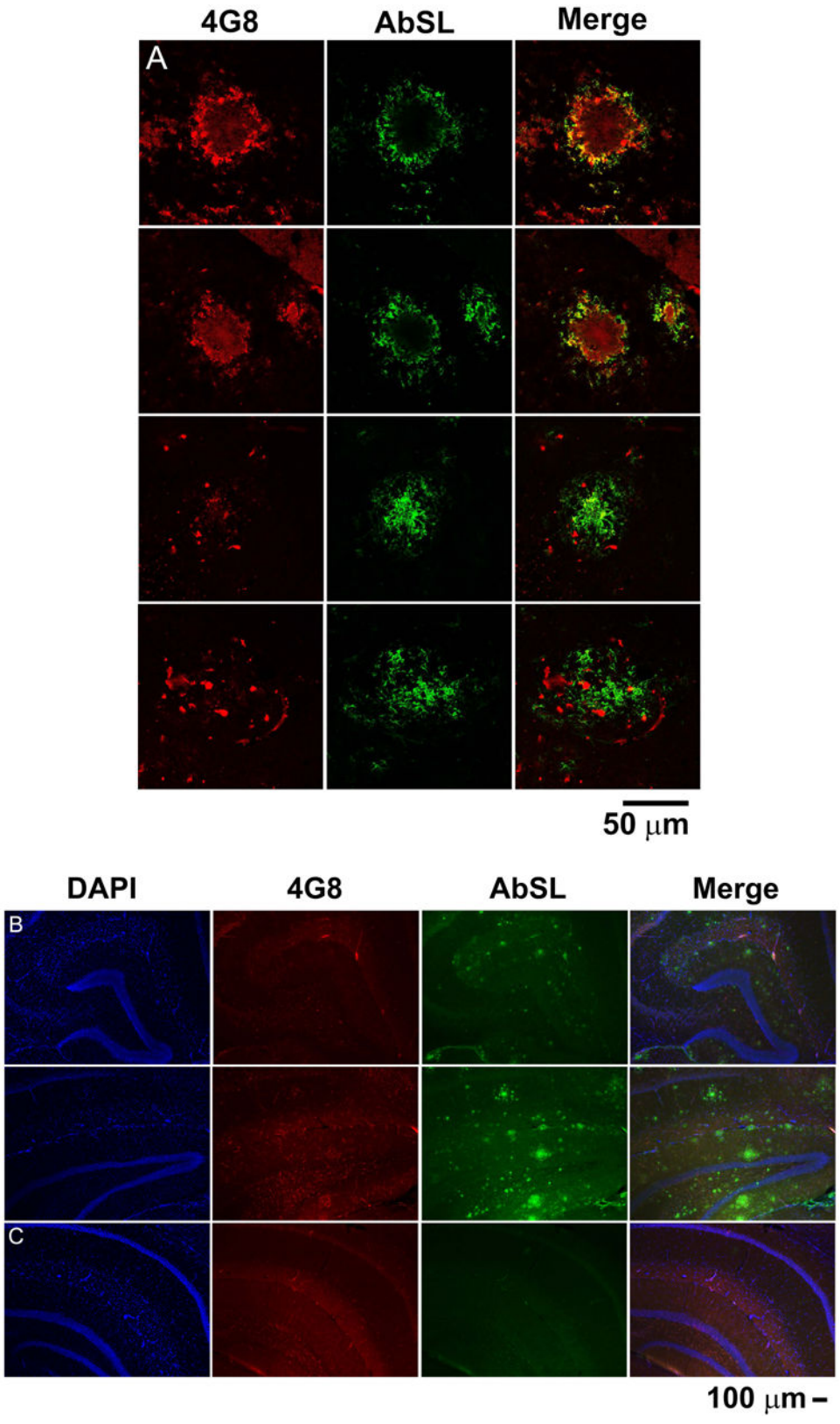

Figure 6.

AbSL antiserum stains distinct pathological amyloid features. Brain hemispheres were prepared from 15 month old WT (C57BL/6) or APP/PS1 mice. Tissue samples were stained with 4G8 or AbSL primary antibodies and detected with either AlexaFluor 594-labeled (4G8, red) or AlexaFluor 488-labeled (AbSL, green) secondary antibodies. Separately stained samples were imaged with either confocal (Panel A) or epifluorescence (Panels B, C) microscopy. Panel A shows four separate sites of amyloid accumulation in 15 month old APP/PS1 brain samples and their reactivity to 4G8 or AbSL. Panel B shows two hippocampal slices obtained from a 15 month old APP/PS1 mouse and stained with DAPI (nuclei, blue), 4G8 (red), or AbSL (green). Panel C is the same staining protocol for a hippocampal slice from a 15 month old WT mouse.

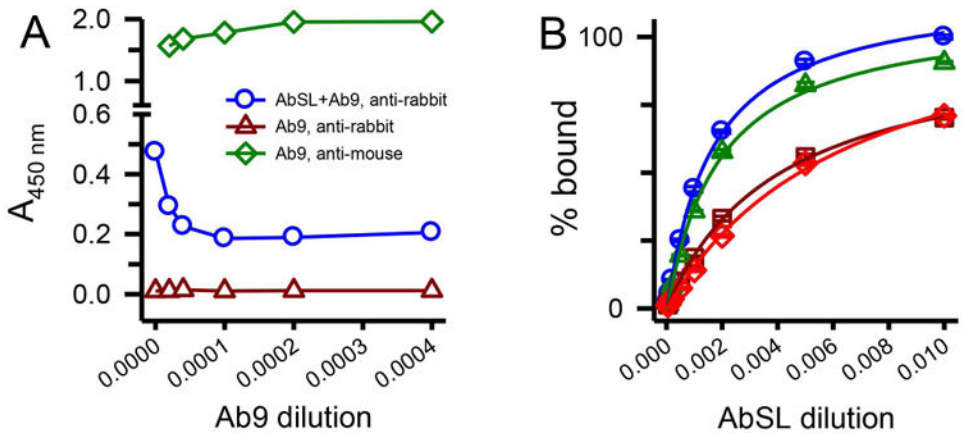

Figure 7.

An N-terminal Aβ antibody partially hinders AbSL binding to protofibrils. Panel A. ELISA plates were coated with SEC-isolated Aβ protofibrils (18 ng/well) and treated with premixed primary antibody solutions containing AbSL (1:1,000) and varying dilutions of Ab9 (2,500-50,000; 0.1-2 μg/mL). Ab9 dilutions are represented on the x-axis as the inverse value of the dilution. Detection of primary antibodies AbSL and Ab9 was done with secondary antibodies anti-rabbit IgG-HRP (for AbSL, blue circles) or anti-mouse IgG-HRP (for Ab9, green diamonds). No detection of Ab9 was observed when anti-rabbit IgG-HRP was used as the secondary antibody (dark red triangles). Panel B. Immunoplates were coated with Aβ protofibrils (18 ng/well) and treated with premixed primary antibody solutions. These solutions contained increasing dilutions of AbSL (100, 500, 1,000, 2,000, 5,000, 10,000, and 20,000) either in the absence (blue circles) or presence of constant amounts of Ab5. Repeated experiments were done at constant Ab5 dilutions of 1:10,000 (green triangles), 1:2,000 (dark red squares), and 1:1,000 (red diamonds). Each experiment determined AbSL binding in the absence of Ab5. Data points (± SEM) represent the average of n=3 trials for each Ab5 dilution and n=12 trials for AbSL alone. Antibody binding on the y-axis is presented as percent A_{450} of the highest AbSL concentration (1:100) in the absence of Ab5.

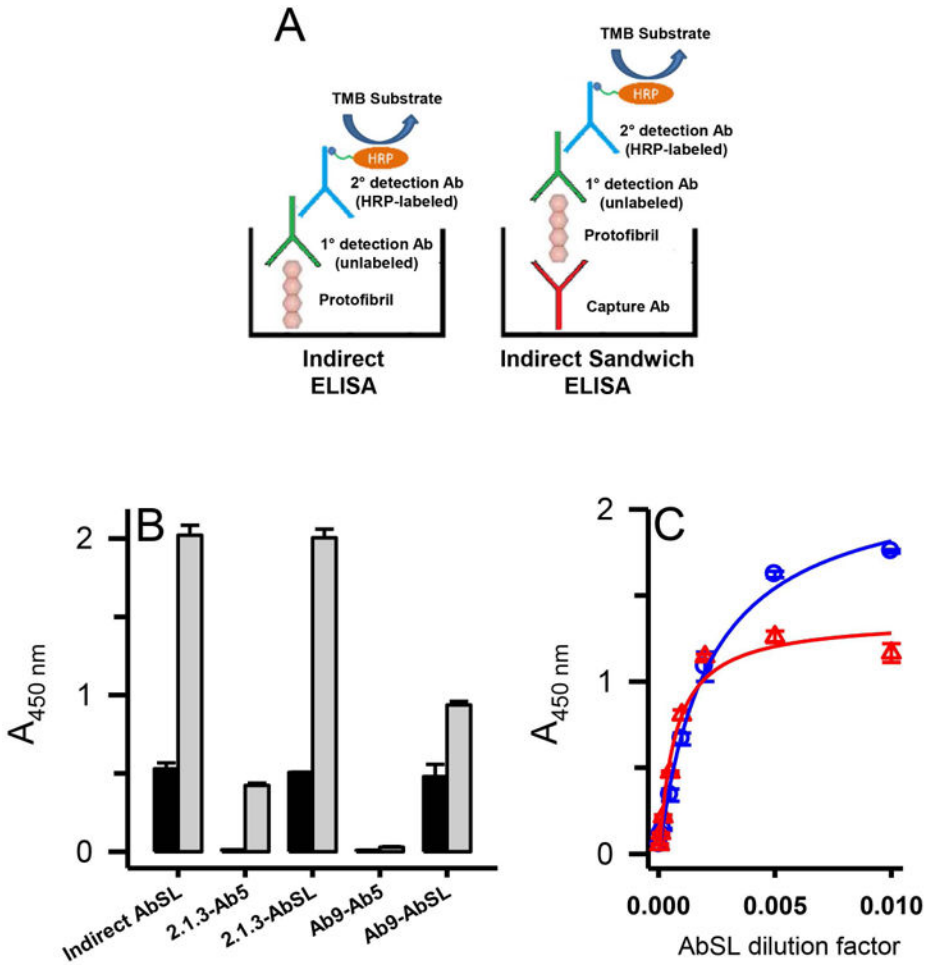

Figure 8.

Conformational epitope on Aβ42 protofibrils for AbSL partially involves the N-terminal region. Panel A. Schematics are shown for the principal ELISA paradigms used for AbSL antibody testing, which include an indirect ELISA and an indirect sandwich ELISA. The latter system used either an HRP-conjugated Ab5 detection antibody (Terrill-Usery *et al.* 2016) or an HRP-conjugated secondary detection antibody when AbSL was used as the primary detection antibody. Panel B. Various combinations of capture and detection antibodies were tested in the indirect sandwich ELISA paradigm. The capture antibody is listed first and the detection antibody second (e.g. 2.1.3-Ab5). ELISA plates were coated with capture antibodies Ab2.1.3 (5 μg/mL) and Ab9 (1 μg/mL) for the indirect sandwich ELISA, which was carried out as described in the Methods. Aβ42 protofibrils (18 ng/well) were added to the capture antibodies followed by various detection antibodies. Background controls (no Aβ42) are shown in the black bars while Aβ42 samples are shown in white bars. Sample data are the mean of n = 4 replicates ± SEM. Panel C. Immunoplates were coated with capture antibodies Ab2.1.3 or Ab5 as described in Panel B. Aβ42 protofibrils (45 ng/well) were added and detected with varying dilutions of AbSL (100-20,000). Sample data are the mean of n = 3 replicates ± SEM and were fit to a 3-parameter single rectangular hyperbola equation.

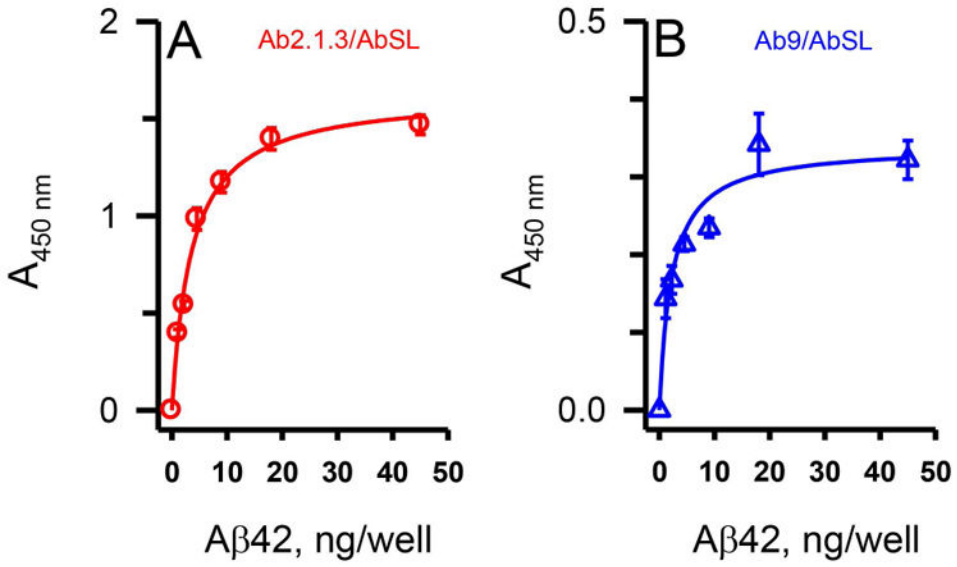

Figure 9.

AbSL binding site is proximal to, but distinct from, the N-terminal Aβ antibody binding site. Panel A. Utilizing the indirect sandwich ELISA format detailed in Figure 8A, increasing amounts of Aβ42 were added to immunoplates previously coated with primary antibodies Ab2.1.3 (Panel A) or Ab9 (Panel B). Detection was accomplished with AbSL antiserum followed by an anti-rabbit IgG-HRP secondary detection antibody. Sample data points are the mean of n = 3 replicates ± SEM and demonstrate a similar affinity of AbSL for protofibrils even in the presence of Ab9.

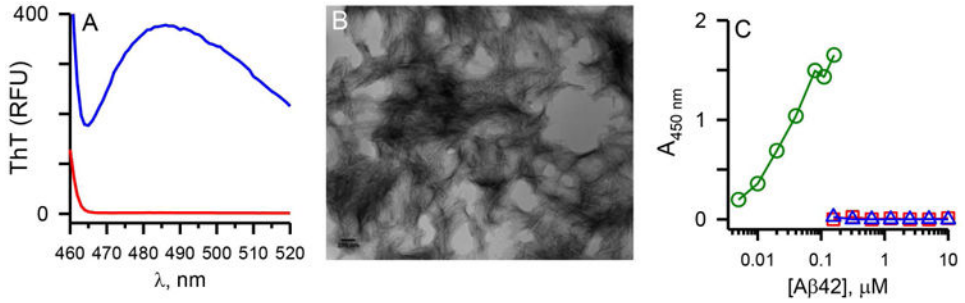

Figure 10.

AbSL does not recognize either monomeric or aggregated Aβ25-35 peptide. SEC-purified Aβ25-35 monomers were allowed to aggregate as described in the Methods. Panel A. ThT measurements of aggregated Aβ25-35 (blue line) and ThT control (red line). Panel B. TEM image of aggregated Aβ25-35 applied to a copper-formwar grid. The scale bar is located in the lower left-hand corner (200 nm). Panel C. Indirect ELISA in immunoplates coated with increasing concentrations of monomeric (red squares) or aggregated (blue triangles) Aβ25-35 peptide or isolated Aβ42 protofibrils (green circles). AbSL (1:5000 dilution) was used as the primary antibody and the ELISA was conducted as described in the Methods.